Journal of Information Systems Engineering and Management
2025, 10(4)
e-ISSN: 2468-4376
https://jisem-journal.com/

Research Article

Electrochemical Simulation and Voltammetric Analysis of Novel Inhibitors for Carbon Steels

Fatiha Chelgham [1,2*], Khadra Mokadem [1], Yamina Benkrima [3], Souheyla Boudjema [4],Amira Ouakkaf [5], Mounira Chelgham [6], Sanaa El korso [4]

[1] Laboratoire de Valorisation et Promotion des Ressources Sahariennes, Université Kasdi Merbah, Ouargla - 30000, Algerie.
[2] Faculté des hydrocarbures, énergies renouvelables, science de la terre et de l'univers, Université Kasdi Merbah, Ouargla-30000, Algerie.
[3]Ecole Normale Supérieure de Ouargla, 30000 Ouargla, Algeria

[4]Département de chimie, Laboratoire de catalyse et synthèse en chimie organique, Univesité de Tlemcen, Tlemcen, Algérie.
[5]Faculté des sciences exactes, Université Mohamed Khider, Biskra,07000, Algerie.
[6]Développement des énergies nouvelles et renouvelables dans les zones arides et sahariennes, LENREZA, P.O. Box 511, Ouargla 30 000, Algeria
*Email: fchelgham@gmail.com

ARTICLE INFO

Received: 05 Jul 2025

Revised: 21 Oct 2025

Accepted: 24 Nov 2025

ABSTRACT

Pipelines are a type of industry infrastructure used for water transportation or in The oil and gas industry. Many pipes made of carbon steel that meets API specifications and comes in various grades are currently used in the oil and gas industry. The American Petroleum Institute's (API) N80 corrosion behavior and Grade B steels in aquifer water (albian), was examined in this study in relation to the effects a Novel Inhibitors of polyoxometalates (PW_{11}/ZrO_2) and ($AgPW_{11}/SiO_2$). The physical, structural properties of This nanocomposites are effectively investigated with XRD crystallography, and FTIR spectroscopy . Polarization curves and electrochemical impedance spectroscopy were used to assess each compound's inhibitory efficiency for the electrochemical investigation we carried out on an experimental test bench. Both inhibitors were anodic, according to polarization studies.

Keywords: PW_{11} /ZrO_2, $AgPW_{11}$ /SiO_2, Albian water ,Corrosion, Carbon Steel

INTRODUCTION

Steel is divided into four categories: mild steel (0.10–0.2%), medium C (0.3–0.6%), low C (0.2–0.3%), and high C (0.6–1.7%). Steel is widely used in many facets of human existence, including manufacturing, transportation, oil and gas, Corrosion is one of the most engineering-defying problems that the steel industry faces, despite its importance and profitability [1]. The integrity of metals, like carbon steel utilized in pipeline networks, might be severely harmed by generated water, leading to significant corrosion issues [2]. However, oil pipeline breakdowns result in significant financial losses [3,4] , and firms spend millions of pounds annually to fix damage [5,6].
According to Reham et al. [7] , and Vel´azquez [8] the American Petroleum Institute's (API) N80 carbon and API 5L grade b is typically utilized as the primary building materials used in the petroleum industry for transportation pipes and downhole tubes.

Typically, corrosion issues are linked to equipment maintenance and operating issues. Therefore, it is crucial to prevent corrosion in metals used in industrial and petroleum-related applications,

Journal of Information Systems Engineering and Management
2025, 10(4)
e-ISSN: 2468-4376
https://jisem-journal.com/

Research Article

particularly in acidic media [9] and Water media [10]. Among the many strategies to stop or minimize damage or deterioration of the metal surface, corrosion inhibitors are among the most effective and practical in the oil and gas sector. [11,12]. High inhibition efficacy, low cost, low toxicity, and ease of manufacture are the benefits of employing as corrosion inhibitors [13,14].

The kind and concentration of the acid, temperature, dissolved organic or inorganic contaminants, and the type of metal being protected are some of the variables that affect the choice of appropriate inhibitors [15].
According to recent research, adding nanoparticles can increase their resistance to abrasion,
like study Bargout et al. [16] show that SiO2 nanocomposites have recently greatly increased metals' resistance to corrosion. may successfully prevent corrosion on metals in a variety of conditions, including seawater. This protection can be obtained in a number of ways: spin coating, electrochemical, etching, or dip coating
Del Ángel-López and associates [17] Thecreation of a ZrO2-SiO2 nanocomposite material for AISI 1018 carbon steel corrosion protection is presented in this study. verified that the mechanical characteristics and resistance to degradation were enhanced by the hybrid coating produced particles.
IN [18] The coated samples were tested in a 3.5% NaCl solution in order to assess the protective capabilities of silica SiO2 and zirconia ZrO2 nanoparticles in epoxy coatings. The corrosion test's findings demonstrated that both of these pigments had better mechanical qualities and anti-corrosion effects than traditional epoxy coatings, which significantly raised the produced coating's anti-corrosion effectiveness.
To enhance the corrosion resistance of API N80 and API Grade B steel in Albian water gathered from the region of Haoud-Berkaoui , which is roughly About 100 kilometers west of Hassi-Messaoud, Algeria, superhydrophobic nano-PW_{11}/ZrO2 and AgPW11/SiO_2 inhibitors were designed and manufactured. electrochemical behavior was examined using electrochemical impedance spectroscopy (EIS) and potentiodynamic polarization (PP).
In order to improve the corrosion behavior of API N80 and API Grade B steel in albian water (aquifer water) collected from the Haoud-Berkaoui area, which is roughly 100 km west of Hassi-Messaoud (Algeria), We prepare a new composites ofnano-PW_{11}/ZrO_2 and AgPW11/SiO2 inhibitors were designed and manufactured electrochemical behavior In order to improve the corrosion behavior of API N80 and API Grade B steel in albian water , We prepare a new composites ofnano-PW11/ZrO2 and AgPW11/SiO2 inhibitors were designed and manufactured. electrochemical behavior was examined utilizing (PP)and (EIS) methodes.

EXPERIMENTAL

Nanocomposites synthesis

Tungtophosphoric acid:(H7PW11 O39 ,n H2O) noted PW11:

36.25 g $Na_2O_4W_{11}$. $2H_2O$ and 2.84 g of HNa_2O_4P are dissolved in 75mL of distilled water. The solution is stirred for 30 min with reflux heating (80-90°C) and titrated to pH 4.8 using strong HNO3 and vigorous stirring. The heteropolyanion is then separated into a dense bottom layer by liquid-liquid extraction using 40mL acetone after the volume has been cut in half by evaporation. The extraction process is continued until there are no nitric ions visible in the acetone extract ($FeSO_4$ ferrous sulfate test). Following the acetone extracts' dry evaporation (in air), solid sodium salt is produced as hydrate ($15–20H_2O$).

$Ag_7PW_{11}O39$. nH_2O noted AgPW:

5.36 g of $H_7PW_{11}O_{39}$. nH2O dissolved in 50 mL volumetric flask filled with 50 mL of pure water under stirring (until completely dissolved), then weigh 2.37 g $AgNO_3$ dissolved in 50 mL distilled water and add the $AgNO_3$ solution dropwise to the solution using a Pasteur pipette, while the mixture is stirred

Journal of Information Systems Engineering and Management
2025, 10(4)
e-ISSN: 2468-4376
https://jisem-journal.com/

Research Article

until the $AgNO_3$ solution is complete. The mixture is then subjected to ultrasound for 50 min. The resulting solution is centrifuged and the solid separated. The solid is dried at 50°C.

Synthesis of PW_{11}/ZrO_2:

A solution of 12.12g ZrO_2 in 25ml nBu OH is stirred for 1h at 80°C. After that, the mixture is allowed to cool to ambient temperature.. The acidity of the mixture is adjusted to 2 using HCl. The resulting solution is added drop wise to the solution of (PW_{11}): an appropriate mass of PW_{11} in 25mL of nBuOH and 10mL of distilled water. The solution is left to stir for 3h until a gel is formed. After gelation, the solid is filtered and air-dried for 24 h. The gel is then dried and calcined at 350°C for 4 h. The inhibitor prepared by this sol-gel method is named as follows: 20% PW_{11}/ZrO_2.

Synthesis of Ag PW/SiO_2:

These materials are prepared by impregnation with an aqueous solution containing the appropriate amount of HPAs to obtain samples with the desired weight percentage of POM to supporting oxide (1g SiO2). The suspension was kept under constant stirring at 50°C for 1h, then for ten hours, the solution was dried at 70°C.. The resulting materials were calcined in air at 200°C for 5h.

The resulting material is named as follows: 20% AgPW/SiO2

Characterization of Chemical Structure

In this study, was used to functional groups in the chemical structure are identified using Fourier Transform Infrared Spectroscopy (FTIR). a PW_{11}/ZrO_2 and $AgPW_{11}/SiO_2$. The principle of this technique is based on the vibrations of molecules when irradiated by an electromagnetic wave in the infrared range from 0.8 µm to 1000 µm.

The crystalline structures of the Both nanoparticles , were assessed through X-ray diffraction (XRD)

Material and solution

The pipeline carbon steel (CS) , was tested in accordance with American Petroleum Institute (API) N80 and grades B [8, 20], were examined in the current investigation using its cross-sectional area of 1 cm^2. In the petroleum industry, flow lines and transmission pipes are often built using API N80 and Grade B CS as the primary building materials [19].

The characteristics of the generated water, which has an average pH of 7.79, as follows :

Ca^{+2} = 175.56 mg/l , Mg+2= 92.82 mg/l , Na^{+} = 284.28 mg/l , K+ =33 mg/l , Cl^{-} =526.85 mg/l , SO_4^{2-} =561.14 mg/l , HCO_3^{-}=150.14 mg/l , NO_3^{-}= 11.85 mg/l

To help comprehend the chemical makeup of the albian water utilized in the studies

Electrochemical Measurements

The corrosion inhibition of Carbon Steel in albian water with and without varying concentrations of PW_{11}/ZrO_2 and $AgPW_{11}/SiO2$ has been studied utilizing methods like Potentiodynamic polarization (PP) and electrochemical impedance spectroscopy (EIS),

Electrochemical tests were conducted at 25°C using a Potentiostat/Galvanostat Type PGZ 301 connected to a PC running VoltaMaster-4 software.

In a traditional three-electrode cell, electrochemical measurements were performed. The working electrode (WE) had a 1 cm^2 section made of API N80 and API 5L Grade B CS , A platinum rod served as the counter electrode, while a saturated calomel electrode (SCE) served as the reference electrode.

The inhibitor (PW_{11}/ZrO_2 - $AgPW_{11}/SiO2$) was present in the test water solutions in varying quantities. An electrode that had been mechanically polished was utilized for every measurement. Emery sheets of progressively finer grades (200-2000 grade) were used for polishing.The polarization curves, also known as The Tafel plots were performed with an open circuit potential scan rate of 30 mV/min and a potential range of -300 to -900 mV. Room temperature was used for the electrochemical measurements.

The method employed was (EIS) measurements were made between 10 mHz and 100 kHz using an excitation AC signal with an amplitude of 10 mV.

Journal of Information Systems Engineering and Management
2025, 10(4)
e-ISSN: 2468-4376
https://jisem-journal.com/

Research Article

RESULTS AND DISCUSSION

Structural analysis by X-ray diffraction (XRD):

XRD characterization can be utilized to ascertain the different crystalline phases present in each inhibitor.

X-ray diffraction profiles of the initial phosphotungstic acid as well as figure 1 shows the comparable nanocatalysts recorded at angles ranging from 2θ = 2.5 to 80 degrees. The main diffractions of PW11crystalline with a Keggin structure (PW12O403-) are observed at angles 2θ: 10.2 ° - 14.5 ° - 17.9 ° - 20.7°- 22 ,2 °- 29.5 ° - 31.3 ° and 34.5 ° [21].

Figure .1 shows diffractograms of the supported materials. The diffractograms of the active phases PW11 and AgPW are shown for comparison. The produced inhibitors' X-ray diffraction pattern features are comparable to those of the corresponding supports reported in the literature [22, 23].

Fourier transform infrared (FTIR) analysis:

FTIR spectra of PW11-based nanoparticles (Figure 2) showed characteristic peaks of [PW11O39]7- anions , for example, W-Oc-W (715-741 cm-1), W-Ob-W (879-907 cm-1), W-Od (861-966 cm-1), and P-Oa (1061-1075 cm-1). The bands corresponding to the [PW11O39]7- groups in the inhibitors suppressed on SiO2 either, were also observed (Figure 2). 728-740 cm-1 (W-Oc-W), 869-910 cm-1 (W-Ob-W), 965-971 cm-1 (W-Od) and 1012-1020 cm-1 (Si-Oa).

An oxygen atom that links two trimetallic groups is called an Oa in the Keggin unit; an oxygen atom that links two octahedral MoO6 within the trimetallic group is called an Oc; and an Od is assigned to the terminal oxygen atoms [24, 25].

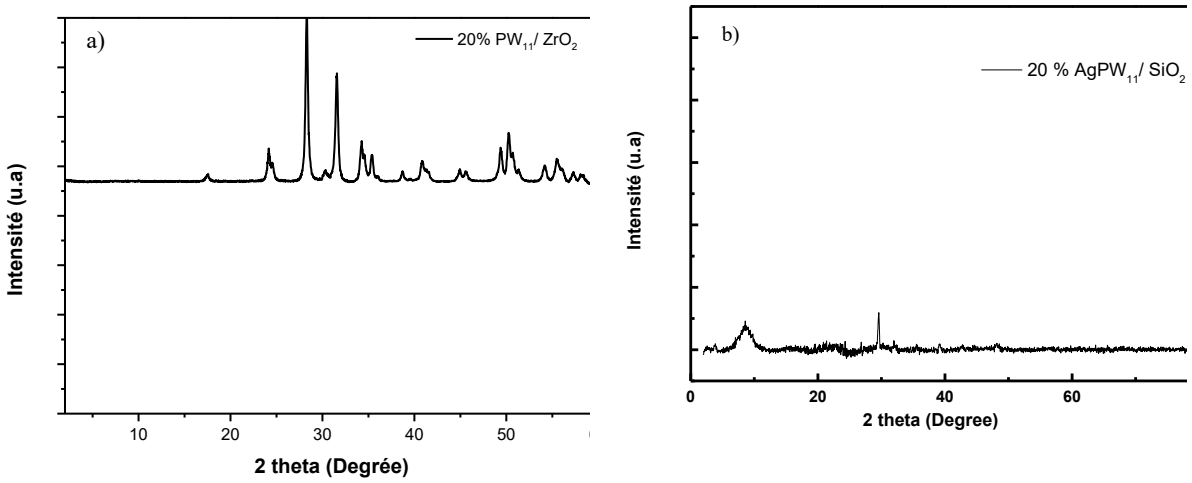

Figure .1. X-ray diffractograms of prepared inhibitors.

Journal of Information Systems Engineering and Management
2025, 10(4)
e-ISSN: 2468-4376
https://jisem-journal.com/

Research Article

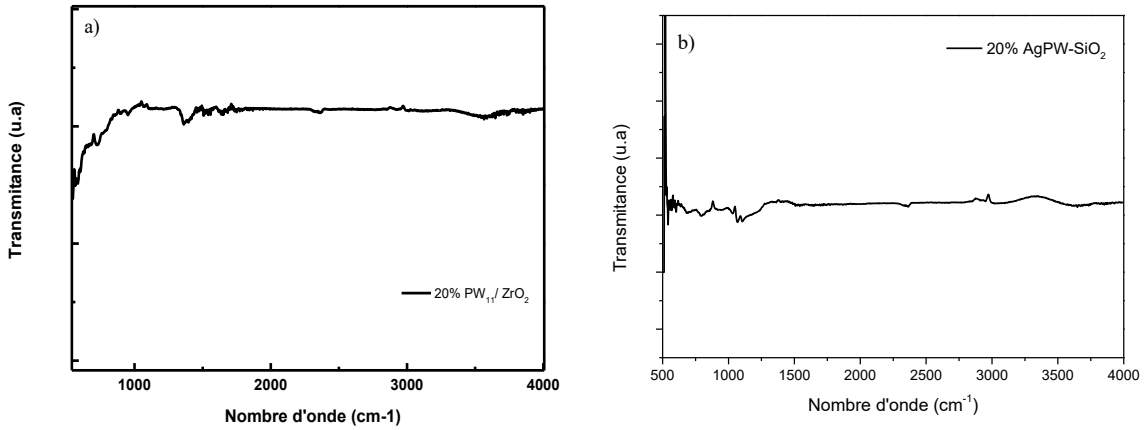

Figure .2.FTIR spectra of prepared materials**.**

Measurements of potentiodynamic polarization

In this part of the study, we evaluated the potentiodynamics of API Grade B and API N80 steel at different concentrations of AgPW11/SiO2 or PW11/ZrO2 in an albian water medium. 25°C, for forty minutes, the samples were exposed to the corrosive media.. Figure 2 displaysthepolarization curves that were produced. The percent inhibition efficiency (IE%) wascomputed using the following formula [26]:

$$E\% = (1 - \frac{i}{i_0}) \times 100 \text{ .....(1)}$$

where io and i, respectively, are the unconstrained and inhibited corrosion current densities.

The values of the inhibitory efficiency (E%) and corrosion rate (CR) derived from

the values of Ecorr, and as the concentration of PW_{11}/ZrO_2 rises, the corrosion current polarization experiments for various PW_{11}/ZrO_2 concentrations in albian water are displayed in Table 3. There are two components for every curve in figure 3-a). There is an anodic component that symbolizes the oxidation of the steel and a cathodic component that reflects the steel's surface proton reduction reaction. In the anodic portion, the oxidation current densities fall when PW_{11}/ZrO_2 is added, but the anodic partial current decreases less when the inhibitor is added. PW_{11}/ZrO_2 can be categorized as an anodic inhibitor in albian water since this clearly shows that it has an anodic impact.

According to the data analysis in Table 1, the addition of PW_{11}/ZrO_2 alters densities (i_{corr}) drop; this decline in current densities is more noticeable at high inhibitor concentrations. A passive coating forms on the metal surface when the inhibitor is present, as evidenced by the observation that E(%) increases with increasing inhibitor concentration, reaching a peak of 87% at 20 ppm of PW11/ZrO2 [27, 28].

Lastly, we observe that the inhibitor PW_{11}/ZrO_2 provided good protection in albian water at all concentrations; this finding supports that of Abdollahi et al.[29]

Figure 3-b displays the steel anodic and cathodic polarization curves in Albian water at different concentrations of ($AgPW_{11}/SiO_2$). These data show that when the concentration of AgPW11/SiO2 rises, the density of corrosion current (icorr) drop in the presence of the inhibitor. and that the inhibitor's concentration causes E (%), the inhibitory efficiency to rise, peaking at 73% at 40 ppm of AgPW11/SiO2. We think that the inhibitor is adhering to the metal surface because of this [32, 33].

Additionally, Tafel ba and bc's anodic and cathodic slopes alter when $AgPW_{11}/SiO_2$ is added, and the values of Ecorr move toward the greatest positive values. These observations imply that the $AgPW_{11}/SiO_2$ inhibitor also possesses anodic inhibitory qualities.

Figure 4 displays The curves of cathodic and anodic polarization of API Grade B steel in an albian water solution with the ideal $PW_{11}/ZrO2$ and $AgPW_{11}/SiO_2$ concentrations. It is clear that the cathodic and anodic curves were moved to a morepositive potential region when the inhibitor was present, and that the shift was influenced by the inhibitor's concentration. The results of the CR and E% calculations are shown in Table 2.

Journal of Information Systems Engineering and Management
2025, 10(4)
e-ISSN: 2468-4376
https://jisem-journal.com/

Research Article

Table4 shows that when PW_{11}/ZrO_2 and $AgPW_{11}/SiO_2$ are present at optimal concentrations, the Ecorr values shift in a noble direction [34, 35]. This observation unequivocally demonstrates that these inhibitors function as anodic type by controlling both cathodic and anodic processes.

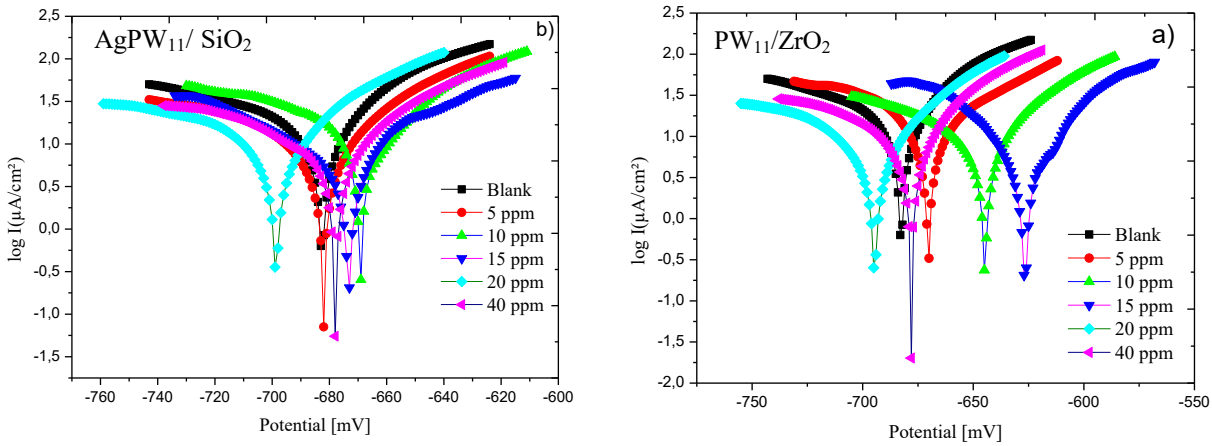

Figure 3. API N80 pipe polarization curves in albian water at different concentrations: a) PW_{11}/ZrO_2 , b) $AgPW_{11}/SiO_2$.

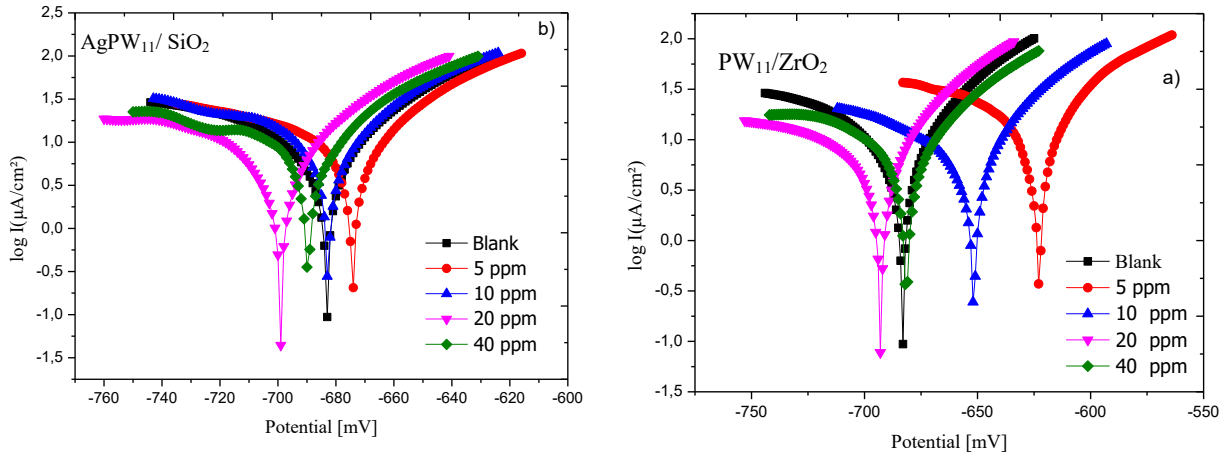

Figure . 4. API Grade B pipe polarization curves in albian water at different concentrations: a) PW_{11}/ZrO_2 , b) $AgPW_{11}/ SiO_2$

Table 1. Potentiodynamic polarization parameters for $PW_{11}/ZrO_2AgPW11/ SiO_2$ inhibitors of API N80 in water of albian.

Journal of Information Systems Engineering and Management
2025, 10(4)
e-ISSN: 2468-4376
https://jisem-journal.com/

Research Article

	Inhibitor conc. ppm)	CR (µm/y)	E corr (mv)	i_{corr} (µA/cm²)	-b_c (mV)	b_a (mV)	Rp (kohm.cm²)	E (%)	
PW_{11}/ZrO_2	Blanc	198.3	-682.5	16.9566	122.8	50.3	0.69084	-	
	5	147.3	-670.3	12.6009	68.7	71.3	0.83008	**25.68**	
	10	100.3	-644.7	8.5821	95.1	49.3	1.26	**49.38**	
	15	100.3	-627.0	3.4190	30.9	31.1	1.80	**79.83**	
	20	25.75	-694.5	2.2019	24.4	19.5	1.58	**87.01**	
	40	81.65	-678.0	6.9814	73.7	37.2	1.25	**58.82**	
AgPW11 / SiO_2	Blanc	198.3	-682.5	16.9566	122.8	50.3	0.69084	-	
	5	103.8	-682.1	8.8792	82.9	46.1	1.17	**47.63**	
	10	64.59	-668.7	5.5227	62.4	30.3	0.89494	**67.43**	
	15	60.00	-673.1	5.1302	61.1	48.4	1.48	**69.74**	
	20	61.24	-698.6	5.2361	39.9	29.7	1.08	**69.12**	
	40	53.50	-677.7	4.5745	50.4	29.1	1.27	**73.02**	

Table 2. Potentiodynamic polarization parameters for PW_{11}/ZrO_2 and AgPW11/ SiO_2 inhibitors of API Grade B steel in albian water**.**

	Inhibitor conc. (ppm)	CR (µm/y)	E corr (mv)	i_{corr} (µA/cm²)	-b_c (mV)	b_a (mV)	Rp (kohm.cm²)	E (%)
PW_{11}/ZrO_2	Blanc	148.6	-683.1	12.7066	159.5	62.8	1.39	-
	5	131.6	-623.1	11.2542	84.3	47.3	0.88024	**11.43**
	10	102.5	-651.8	8.7683	157.1	53.5	1.63	**30.99**
	20	81.52	-692.9	6.9704	147.9	47.2	1.78	**45.14**
	40	57.01	-681.4	4.8749	59.2	38.7	1.43	**61.63**
AgPW11/ SiO_2	Blanc	148.6	-683.1	12.7066	159.5	62.8	1.39	-
	5	117.3	-674.1	10.0323	124.8	50.9	1.15	**21.04**
	10	99.99	-682.6	8.5497	73.1	45.2	1.08	**32.71**
	20	82.62	-699.3	7.0646	99.1	45.7	1.74	**44.40**
	40	52.46	-689.3	4.4860	72.2	29.6	1.222	**64.69**

Electrochemical impedance spectroscopy (EIS)

Electrochemical EIS curves were employed in this study to more accurately evaluate steels' resistance to corrosion.

The API N80 and API Grade B were submerged in albian water for 30 minutes, and EIS measurements were made at various PW_{11}/ZrO_2 and $AgPW_{11}/SiO_2$ concentrations to validate the potentiodynamic polarization results. Figure 4., which displays the Nyquist plots, shows that each spectrum contains a loop whose diameter grows as the concentrations of PW_{11}/ZrO_2 and $AgPW_{11}/SiO_2$ increase. As a result, API N80 steel exhibits the best corrosion resistance at concentrations of 20 and 40 ppm of effectiveness 52.83% and 65.84 %, respectively [27,28].

Table 3 lists the fitted parameters. For both inhibitors, the Rct indicates how difficult it is to charge across the surface's interaction with the electrolyte solution. The corrosive medium's diffusion path lengthens with increasing Rct. $AgPW_{11}/SiO_2$ clearly has a better protective effect than PW_{11}/ZrO_2.

The corrosion behavior of API Grade B steel and both inhibitors was examined using room-temperature electrochemical impedance spectroscopy. Table 4 lists several impedance metrics, including resistance to charge transfer (Rct) and η% . The (Rct) was calculated using the differential in impedance between

Journal of Information Systems Engineering and Management
2025, 10(4)
e-ISSN: 2468-4376
https://jisem-journal.com/

Research Article

the lower and higher frequencies. Figure 5 displays Inhibited and uninhibited steel Nyquist plots in albian water at optimal concentrations of 40 ppm AgPW11/SiO2 and PW11/ZrO2 [34, 35].
The quantity of molecules adsorbed on the surfaces has increased of both steels is most likely the cause of the notable rise in the Rt value that occurs when the concentrations of PW_{11}/ZrO_2 and $AgPW_{11}/SiO_2$ increase [29,30,31].
In fact, the film gets thicker and the capacity of the double layer gets smaller as the inhibitor adsorbs. In the Helmholtz model, the following connection [36] describes the relationship between the deposit thickness and the capacity of the double layer:

$$C_{dl} = \frac{\varepsilon_0 \varepsilon}{e} S \quad \text{.....(2)}$$

where ε represents The dielectric constant of the medium, ε_0 the free-space permittivity, S the electrode's effective area, and e the thickness of the double layer of protection provided by the inhibitors.

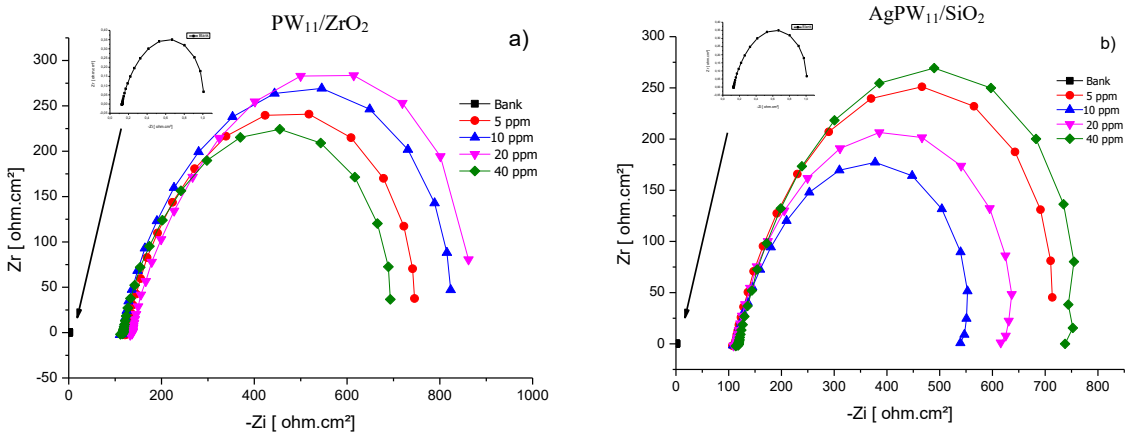

Figure 5. API N80 pipe Nyquist diagrams in Albian water, without inhibitor and at different concentrations of a)PW_{11}/ZrO_2 b) $AgPW_{11}/SiO_2$

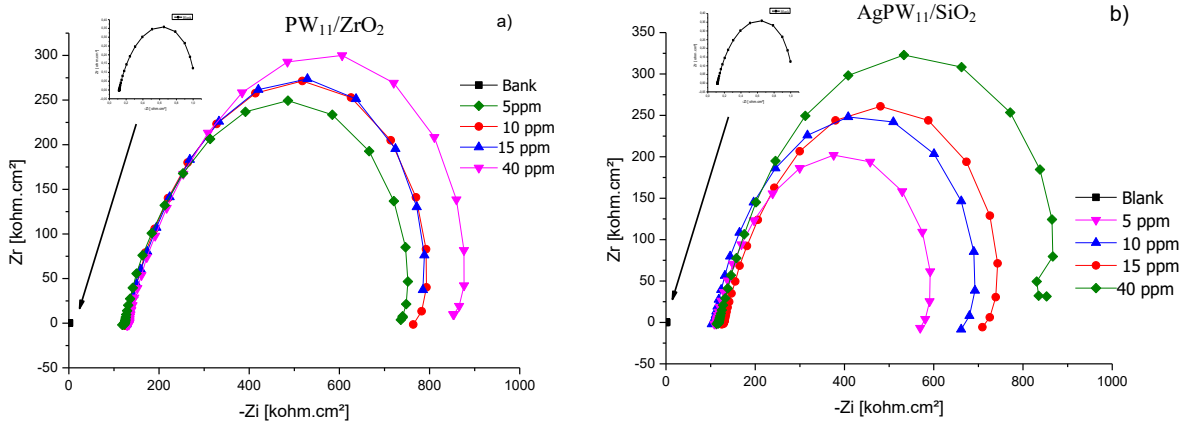

Figure.6. API Grade B pipe Nyquist diagrams in Albian water, without inhibitor and at different concentrations of a)PW_{11}/ZrO_2 b) $AgPW_{11}/SiO_2$

Table.3. EIS parameters of PW_{11}/ZrO_2 and $AgPW_{11}/SiO_2$ of API N80 in Albian water

Journal of Information Systems Engineering and Management
2025, 10(4)
e-ISSN: 2468-4376
https://jisem-journal.com/

Research Article

Conc. (ppm)	R_t (Ωcm²)	C_{dl} (µF cm⁻²)	η %
Blanc	834.4	1.2531	/
PW_{11}/ZrO_2			
5	558.3	0,7096	43.36
10	601.4	0,6609	47.32
20	690.11	0,5911	52.83
40	690.45	0,8870	29.20
$AgPW_{11}/SiO_2$			
5	425.9	0.89777	28.41
10	602.45	0.63381	49.48
20	618.7	0.590991	52.84
40	568.15	0.42879	65.84

Table.4. EIS parameters of PW_{11}/ZrO_2 and $AgPW_{11}/SiO_2$ of API Grade B steel in Albian water

Conc. (ppm)	R_t (Ωcm²)	C_{dl} (µF cm⁻²)	η %
Blanc	793 .6	2. 1678	/
PW_{11}/ZrO_2			
5	656.81	0.91869	57.63
10	718.66	0.83817	61.29
15	718.66	0.88407	61.20
40	635.64	0.85863	72.95
$AgPW_{11}/SiO_2$			
5	118.449	0.778606	64.07
10	129 .133	0.679624	68.63
15	129 .133	0.610024	71.85
40	113.968	0.497707	77 .03

CONCLUSION

This work was new prepared and devoted to the study and evaluation of corrosion inhibitors based on polyoxometalates PW_{11}/ZrO_2 and $AgPW_{11}/SiO_2$ in albian water. To this end, we first prepared the polyoxometalates , then characterized them using DRX and FTIR analysis methods, and finally evaluated their corrosion resistance using the potentiodynamic polarization (PP) and electrochemical impedance spectroscopy(EIS) . The characterization results confirm the structure of PW_{11}/ZrO_2 and $AgPW_{11}/SiO_2$.

The two PP and EIS methods used enabled us to conclude that for API 5CT N 80 , the best inhibitor was PW_{11}/ZrO_2, with an efficiency of 87%. For API 5L Grade B , the best inhibitor was $AgPW_{11}/SiO_2$, with an efficiency of 72%

Journal of Information Systems Engineering and Management
2025, 10(4)
e-ISSN: 2468-4376
https://jisem-journal.com/

Research Article

REFERENCE

[1] Kolotyrkin, J.M. Pitting corrosion of metals. Corrosion 1963, 19, 261.
[2] Benamor, A.; Talkhan, A.G.; Nasser, M.; Hussein, I.; Okonkwo, P.C. Effect of temperature and fluid speed on the corrosion behavior of carbon steel pipeline in Qatari oilfield produced water. J. Electroanal. Chem. 2018, 218.
[3] Peng, C.; Liu, Z.; Wei, X. Failure analysis of a steel tube joint perforated by corrosion in a well-drilling pipe. Eng. Fail. Anal. 2012, 25, 13.
[4] Alamilla, J.L.; Sosa, E.; Sánchez-Magaña, C.A.; Andrade-Valencia, R.; Contreras, A. Failure analysis and mechanical performance of an oil pipeline. Mater. Des. 2013, 50, 766.
[5] Tang, P.; Yang, J.; Zheng, J.; Wong, I.; He, S.; Ye, J.; Ou, G. Failure analysis and prediction of pipes due to the interaction between multiphase flow and structure. Eng. Fail. Anal. 2009, 16, 1749.
[6] Zhang, M.M.; Katz, J.; Prosperetti, A. Enhancement of channel wall vibration due to acoustic excitation of an internal bubbly flow. J. Fluids Struct. 2010, 26, 994.
[7] Wahba, R.H.; El-Sonbati, A.Z.; Diab, M.A.; Gomaa, E.A.; El-Nahass, M.N.; Abdallah, Y.M. Electrochemical corrosion performance of N80 steel in acidized 10% HCl medium using 4-methyl-1-phenyl-3-(p-tolyldiazenyl)-2,3-dihydro-1H-pyrrol-2-ol. Heliyon 2025, 11, e42317.
[8] Velázquez, J.C.; Diaz-Cruz, M.; González-Arévalo, N.E.; Solis, U.O.; Tobón, A.C.; Colindres, S.C.; Sierra, R.C. Study on the loss of ductility of the API 5L grade B steel using the isothermal aging process. Results Eng. 2025, 25, 104223.
[9] Khidr, T.T.; Doheim, M.M.; El-Shamy, O.A.A.; Abdelraheem, O.H. Corrosion inhibition of novel prepared cationic surfactants for API N80 carbon steel pipelines in oil industries. Surf. Eng. Appl. Elect. 2013, 5, 1826.
[10] Chelgham, F.; Ouakkaf, A.; Chelgham, M.; Boudjema, S.; Bouzid, N.; Saidi, M.; Taabouche, A.; Hima, A. Study of the corrosion inhibition of API N80 steel by potassium dichromates and 5-methyl-1H-benzotriazol. Prot. Met. Phys. Chem. Surf. 2024, 60, 1022.
[11] Migahed, M.A.; Al-Sabagh, A.M. Beneficial role of surfactants as corrosion inhibitors in petroleum industry: a review article. Chem. Eng. Commun. 2009, 196.
[12] Riastuti, R.; Mashanafie, G.; Rizkia, V.; Maksum, A.; Prifiharni, S.; Kaban, A.; Priyotomo, G.; Soedarsono, J. Effect of Syzygium cumini leaf extract as a green corrosion inhibitor on API 5L carbon steel in 1M HCl. East. Eur. J. Enterp. Technol. 2022, 6, 30.
[13] Abd-El-Naby, B.A.; Abdullatef, O.A.; Khamis, E.; El-Mahmody, W.A. Effect of cetyltrimethylammonium bromide surfactant as novel inhibitor for the corrosion of steel in 0.5 M H_2SO_4. Int. J. Electrochem. Sci. 2016, 11, 1271.
[14] Shafek, S.H.; Ghiaty, E.A.; El Basiony, N.M.; Badr, E.A.; Shaban, S.M. Preparation of zwitterionic ionic surfactants-based sulphonyl for steel protections: experimental and theoretical insights. Z. Phys. Chem. 2023, 237, 1.
[15] Chetouani, A.; Hammouti, B.; Benhadda, T.; Daoudi, M. Inhibitive action of bipyrazolic type organic compounds towards corrosion of pure iron in acidic media. Appl. Surf. Sci. 2005, 249, 375.
[16] Bargout, N.; Kashyout, A.E.H.B.; Ibrahim, M.A.M.; Hassaan, M.A.; Nemr, A.E. Synthesis of SiC–SiO_2–Si nanocomposites from natural resources and waste for corrosion resistance and circular economy. ChemistrySelect 2025, 10, e202405173.
[17] Del Ángel-López, D.; Torres-Huerta, A.M.; Domínguez-Crespo, M.A.; Onofre-Bustamante, E. Effect of ZrO_2:SiO_2 dispersion on the thermal stability, mechanical properties and corrosion behavior of hybrid coatings deposited on carbon steel. J. Alloys Compd. 2014, 615, S423.
[18] Samad, U.A.; Alam, M.A.; Abdo, H.S.; Anis, A.; Al-Zahrani, S.M. Synergistic effect of nanoparticles: enhanced mechanical and corrosion protection properties of epoxy coatings incorporated with SiO_2 and ZrO_2. Polymers 2023, 15, 3100.

[19] Zhu, S.D.; Fu, A.Q.; Miao, J.; Yin, Z.F.; Zhou, G.S.; Wei, J.F. Corrosion of N80 carbon steel in oil field formation water containing CO2 in the absence and presence of acetic acid. Corros. Sci. 2011, 53, 3156.
[20] Fouda, A.S.; Elmorsi, M.A.; Fayed, T.; Shaban, S.M.; Azazy, O. Corrosion inhibition of novel prepared cationic surfactants for API N80 carbon steel pipelines in oil industries. Surf. Eng. Appl. Electrochem. 2018, 54, 180.
[21] Boudjema, S. Synthèse de polyoxométalates à base de vanadium et/ou de ruthénium. Application à l'époxydation du cyclohexène. University of Tlemcen, 2015.
[22] Xu, L.; Yang, X.; Guo, Y.; Ma, F.; Guo, Y.; Yuan, X.; Huo, M. Simulated sunlight photodegradation of aqueous phthalate esters catalyzed by the polyoxotungstate/titania nanocomposite. J. Hazard. Mater. 2010, 178, 1070.
[23] Ahmadabad, F.K.; Pourayoubi, M.; Bakhshi, H. Novel Keggin-type polyoxometalate nanocatalysts for Michael addition polymerizations. Mater. Chem. Phys. 2017, 199, 79.
[24] Borghese, S.; Louis, B.; Blanc, A.; Pale, P. Design of silver(I)-heteropolyacids: toward the molecular control of reactivity in organic chemistry. Catal. Sci. Technol. 2011, 1, 981.
[25] Qu, X.; Guo, Y.; Hu, C. Preparation and heterogeneous photocatalytic activity of mesoporous H3PW12O40/ZrO2 composites. J. Mol. Catal. A Chem. 2007, 262, 128.
[26] Zhang, Q.B.; Hua, Y.X. Corrosion inhibition of mild steel by alkylimidazolium ionic liquids in hydrochloric acid. Electrochim. Acta 2009, 54, 1881.
[27] Habib, S.; Zafar, S.; Shkoor, M.; Khaled, M.; Hussein, I.A.; Elsadig, M.A.; Dawoud, A.; Shakoor, R.A. Improving corrosion inhibition of steel using polyurethane based composite coatings by incorporating zirconia nanoparticles and novel urea-based inhibitor. Surf. Coat. Tech. 2025, 511, 132316.
[28] Rathi, A.; Kundalwal, S.I. Synergistic effect of ultrasonically assisted exfoliated MWCNTs by ZrO2 nanoparticles on thermo-mechanical and anti-corrosive properties of epoxy nanocomposites. J. Compos. Mater. 2022, 0, 1.
[29] Behnam, A.; Afzali, D.; Hassani, Z. Corrosion inhibition properties of SiO2-ZrO2 nanocomposite coating on carbon steel. Anti-Corros. Methods Mater. 2018, 65, 66.
[30] Akeem, A., B., kayode ,D. ,O., sulaiman ,T.,R. , ayeni ,I. , kolawole ,O., A. , Hefnawy ,M. , ali ,E., Binemran,T.,And andrew edwin ofudje, malachite green adsorption from aqueous medium by chitosan assisted silver nanoparticles (agnps): isotherm and thermodynamics studies, Bull. Chem. Soc. Ethiop. 2025, 39(7), 1283-1299
[31] Mahmoud, Z.H.; Ghadir, G.K.; Al-Tmimi, H.M.; Al-Shuwaili, S.J.; Ami, AA.; Radi, U.K.;
[32] Hameed, S.M.; Mustafa, M.A. Polyaniline/TiO2 nanocomposite for high performance
[33] supercapacitor. Bull. Chem. Soc. Ethiop. 2024, 38, 1177-1188.
[34] Çıtak, B.; Kırsever, D.; Demirkıran, A.Ş.; Boussebha, H.; Ayday, A. The corrosion kinetics of cordierite-based ZrO2 composites obtained from natural zeolite in dilute HCl acid solution. J. Compos. Mater. 2021, 55, 2751.
[35] Ajay, A.V.; Nair, S.S.; Mohan, S.; Vaisakh, Y. Investigation on the influence of nano structured zirconia coating on the corrosion inhibition of SS 304 stainless steel. In: Antony, K.; Davim, J. AM²S. 2018, 203.
[36] Yan, R.; Xue, B.; Wang, C.; Zhang, H.; Yue, Y.; Luo, J. Study on properties of porous SiO2/GO modified polyurethane coatings loaded with corrosion inhibitor. J. Phys. Conf. Ser. 2022, 2200, 012013.
[37] Amiri, S. Enhancement of hydrophobic and anti-corrosive performance of epoxy coatings based on graphene oxide and nano-silica/graphene oxide hybrid. Silicon 2025, 17, 1657.
[38] Bataillon, C.; Brunet, S. Electrochemical impedance spectroscopy on oxide films formed on zircaloy 4 in high temperature water. Electrochim. Acta 1994, 39, 455.